Signature of the Conformational Preferences of Small Peptides: a Theoretical Investigation

Nađa Došlić,* Goran Kovačević, and Ivan Ljubić*

Department of Physical Chemistry, Ruđer Bošković Institute, Bijenička cesta 54, Post Office Box 180, HR-10002, Zagreb, Republic of Croatia

Received: April 2, 2007; In Final Form: June 11, 2007

An extensive computational study of the conformational preferences of *N*-acetylphenylalaninylamide (NAPA) is reported, including conformational and anharmonic frequency analyses, as well as calculations of excitation energies of the four NAPA conformers lowest in energy. Particular attention is paid to the influence of hydrogen-bonding interactions on the relative stability of the conformers, which was found to be very sensitive to both the level of quantum chemical computations and the anharmonic treatment of molecular vibrations. The assignments of the UV spectral peaks are well supported by the multireference CASSCF/MS-CASPT2 calculations. Upon consideration of the second-order Möller−Plesset (MP2) and density functional theory (DFT) structures, overall energetics, and harmonic and anharmonic corrections, we found no conclusive theoretical evidence for the assumed conformational propensity of small model peptides toward extended β-strand structures.

Introduction

In the last couple of years, double resonance IR/UV spectroscopy has emerged as a powerful tool for studying conformational preferences of small peptides containing UV chromophores.[1−9] UV spectroscopy, being sensitive to the chromophore environment, helps identify conformational isomers present in a given sample, while the combination of IR spectroscopy and density functional theory (DFT) calculations allows determination of their geometries. The folding processes in peptides are thought to be governed mainly by hydrogen bonding, whose signature in the fingerprint region of the vibrational spectrum enables identification of a specific conformer. Conformer-specific IR data, available for model systems such as N-Ac-Phe-NH_2 (*N*-acetylphenylalaninylamide or NAPA),[6,7] N-Ac-Trp-NH_2 (*N*-acetyltryptophanylamide or NATA),[3] and N-Ac-X-Phe-NH_2 [X = Gly (glycine), Ala (alanine), Val (valine), or Pro (proline)],[5,8,9] are valuable starting points for size-controlled investigations of intrinsic conformational preferences in peptides.

In this work we plan to investigate the IR/UV double resonance experiments from a theoretical point of view, choosing NAPA (Figure 1) as our model dipeptide system. By employing high-level quantum chemical treatments, we provide an assessment of the anharmonic effects on the relative stability and vibrational frequencies of the NAPA conformers, as well as an insight into the $S_1 \leftarrow S_0$ spectral region of the Phe chromophore embedded in a biological context. By combining these two facets, we hope to shed new light on the intramolecular interactions crucial for shaping the peptide backbone.

Focusing on the IR counterpart of the IR/UV double resonance experiments, previous attempts at assigning the NAPA conformers from the spectra were assisted exclusively by density functional theory (DFT) calculations, viz., the scaled DFT harmonic vibrational frequencies.[6] While scaling of harmonic frequencies is typically effective in simultaneously compensating for the deficiencies of the employed quantum chemical level and the harmonic approximation,[10] in NAPA one might expect to encounter both these issues to a considerable extent. Thus the size of the system allows for calculations with modest basis sets only, while its floppiness points toward significant anharmonic effects. The latter are expected to arise mainly from H-bonding interactions, characterized by broadening and red-shifting of the proton donor (NH) stretching vibrations.[11] Hydrogen bonding is also expected to trigger couplings between localized high-frequency modes and delocalized low-frequency modes of the peptide backbone,[12−14] which may in turn affect the character of the fingerprint amide I, II, and A normal modes, that is, their composition in terms of internal coordinate displacements.

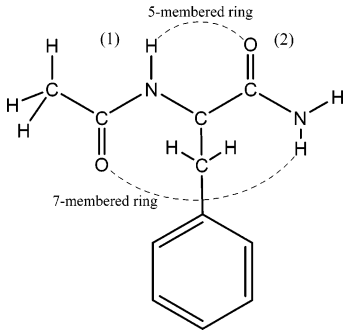

Figure 1. Hydrogen-bonding scheme in NAPA.

In spite of the potentially high impact of anharmonic effects in the case of flexible biomolecules, very few calculations of vibrational spectra beyond the harmonic approximation were performed. Clary and co-workers[15] used the quantum diffusion Monte Carlo method to compute the exact zero-point energy of extremely floppy water complexes with nucleobases. Whereas fairly small anharmonic corrections to the zero-point energy were found, the intermolecular distances were affected significantly. The correlation-consistent vibrational self-consistent field (cc-VSCF) method[16] with analytical force fields was used in studies of peptides[17] and proteins,[18] while ab initio computed potentials were employed for *N*-methylacetamide, glycine, and

* Authors to whom correspondence should be addressed: e-mail nadja.doslic@irb.hr (N.D.) or iljubic@irb.hr (I.L.).

10.1021/jp072565o CCC: $37.00
Published on Web 08/11/2007

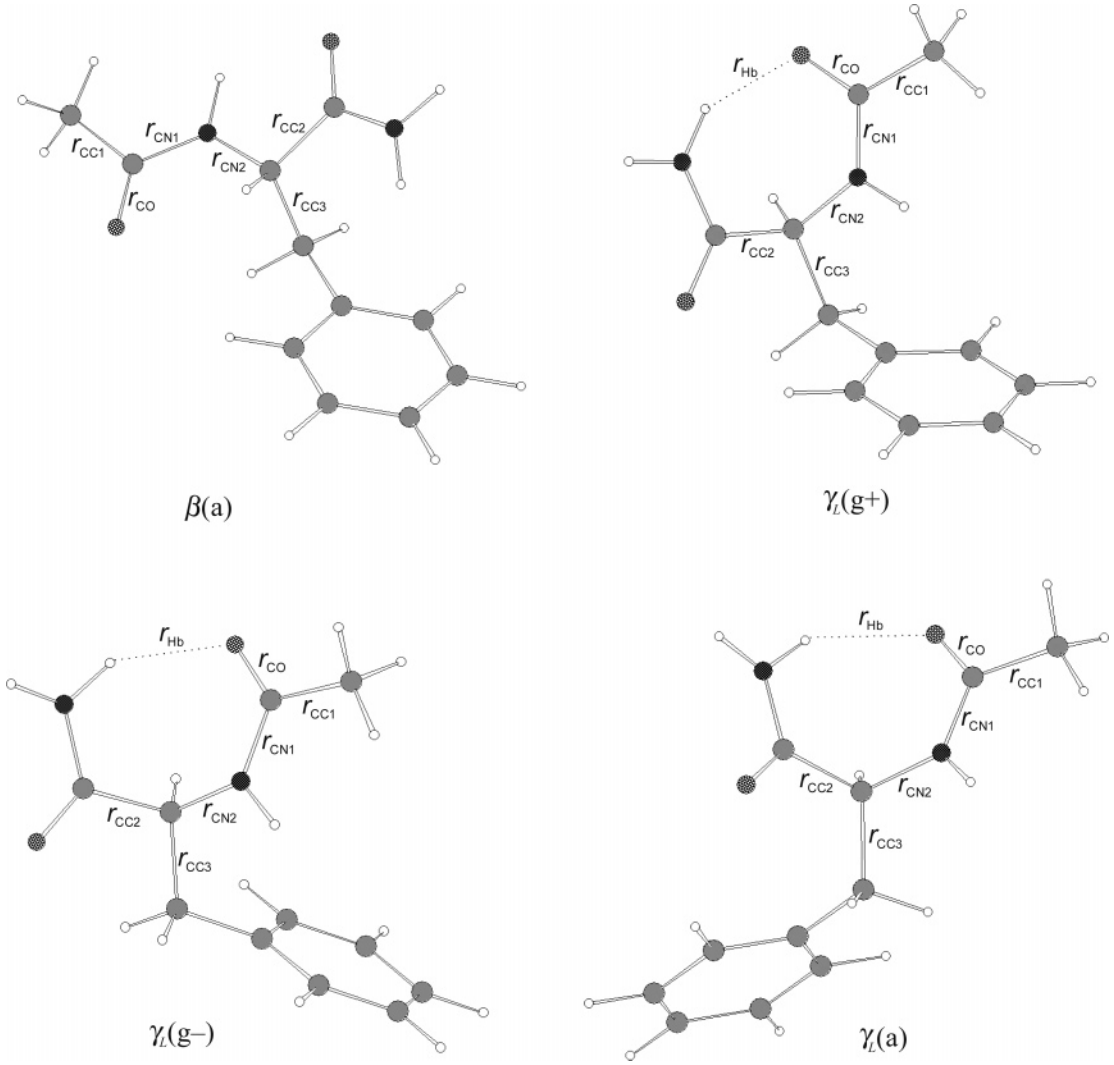

Figure 2. Four low-energy conformations of NAPA according to the Ramachandran classification.

the glycine−water system.[19] It was shown that while anharmonic effects amount to merely 5% in high-frequency hydrogen stretches, they are extremely large in the soft (collective) modes of the molecular framework, where the anharmonic contribution becomes comparable to the harmonic one. However, considering that NAPA has 81 vibrational degrees of freedom and several energetically accessible conformers, cc-VSCF computations at ab initio/DFT evaluated potential grid points are virtually impossible. A viable alternative is provided by the second-order perturbative treatment (PT2) of molecular vibrations,[20,21] which in the case of NAPA is at the very edge of what is presently feasible computationally. Here anharmonic corrections are computed from cubic, diagonal, and semidiagonal quartic force constants by numerical differentiation of the Hessian matrix along normal coordinates. This procedure was tested on a variety of molecules of chemical interest including pyridine, pyrimidine,[20] and prototype H-bonded systems such as acetylacetone.[22] It has proven to be computationally effective, yielding anharmonic frequencies comparable to the cc-VSCF ones,[23] and anharmonic corrections not particularly sensitive to the basis set size.[12,21] In this work we take advantage of these findings and combine DFT harmonic frequencies from several levels with anharmonic corrections computed at a single level of theory.

The UV spectra in the $S_1 \leftarrow S_0$ absorption region of the Phe chromophore were extracted from the IR/UV double resonance experiments by applying the one-color resonant two-photon ionization (R2PI) technique in scanning the UV laser.[6] Three spectral systems were distinguished and assigned to the different NAPA conformers on basis of spectral shifts and Franck−Condon intensities,[6] however, without corroboration via high-level quantum chemistry. Here we plan to obtain the UV excitation properties of various NAPA conformers by means of two state-of-the-art treatments: complete active space self-consistent field method[24] followed by the second-order multi-reference perturbation theory[25] (CASSCF/CASPT2) as well as the time-dependent DFT (TD-DFT) approach.[26] Throughout the past decade the CASSCF/CASPT2 method has in particular evolved as a powerful tool for rationalizing UV/vis spectra of a large variety of molecules,[27] while testing TD-DFT against CASSCF/CASPT2 should be of interest,[28] especially in systems as large as NAPA, where TD-DFT presents a comparatively inexpensive alternative allowing for more extensive basis sets.

Model System

The present theoretical contribution focuses on the UV and IR spectroscopic signature of the four NAPA conformers shown in Figure 2 and is motivated by the availability of high-quality experimental results. Chin et al.[6,7] showed that, among several conformational families, only two are present in the supersonic expansion. According to the Ramachandran terminology,[29] they are classified as (1) the extended β-strand forms supporting a five-membered ring (C5, Figure 1) (NH−C_α−CO) interaction on the same residue and (2) inverse γ-turns (γ_L) exhibiting a

seven-membered ring (C7, Figure 1) backbone conformation. Three structures differing in the orientation of the phenyl ring (Figure 2) were identified in the experiment.[6,7] In the standard terminology these are labeled according to the $N-C_\alpha-C_\beta-C_\gamma$ dihedral angle (χ) as gauche± (g±) for χ close to ±60°, and anti (a) for χ close to 180°.

It is worth noticing that, compared to *N*-methylacetamide (NMA) as a textbook molecule in the study of vibrational coupling between the amide I and amide II modes,[30] the presence of the two peptide groups in NAPA allows study of interaction between the two amide I modes.

Computational Methods

The conformational landscape of NAPA was investigated with the basin-hopping method by use of the AMBER 96 force-field parameter set.[31] The method is implemented in the SCAN program of the TINKER program package, version 4.1.[32] The initial structure of NAPA was subjected to the AMBER 96 force-field geometry optimization before the conformational search was applied. The basin-hopping procedure found 34 distinctive conformers, whose geometries were further optimized by DFT with the Becke-styled three-parameter hybrid functional B3LYP[33] and the inexpensive 3-21G basis set. The geometries of eight of the conformers lowest in energy were then refined at the B3LYP/6-31+G(d) level, whereupon the four most stable conformers, denoted β(a), γ_L(g−), γ_L(g+), and γ_L(a), were singled out. They coincide with those found by Chin et al.[6]

The B3LYP/6-31+G(d) zero-point vibrational energies (ZPEs) and anharmonic frequencies, ν_i, were computed by use of the second-order perturbative treatment as implemented in Gaussian03. In accordance with the original work of Barone,[20] the ZPE is given by

$$\mathrm{ZPE} = \frac{1}{2}(\mathrm{ZPE_H} + \mathrm{ZPE_F}) + \xi_0 - \frac{1}{4}\sum_i \xi_{ii} \qquad (1)$$

where

$$\mathrm{ZPE_H} = \frac{1}{2}\sum_i \omega_i \qquad (2)$$

is the harmonic contribution to the zero-point energy (ω_i are the harmonic frequencies), and

$$\mathrm{ZPE_F} = \frac{1}{2}\sum_i \nu_i \qquad (3)$$

is the anharmonic contribution. The ξ_0 and ξ_{ii} terms are functions in cubic and quartic force constants. With the anharmonic correction defined as $\Delta = \mathrm{ZPE_H} - \mathrm{ZPE_F}$, the following applies to the system under consideration:

$$\xi_0 - \frac{1}{4}\sum_i \xi_{ii} \ll \Delta \qquad (4)$$

In a number of test studies on small molecules it was shown that the anharmonic corrections are not particularly sensitive to the size of the basis set; that is, they converge faster than the corresponding harmonic frequencies.[20,21] We therefore assume that the 6-31+G(d) basis set provides acceptably converged anharmonic corrections, and we combine these corrections with harmonic frequencies obtained at various levels of theory. For the four selected conformers, the geometries and harmonic frequencies were recalculated at the B3LYP/6-31G(d,p) and B3LYP/6-311+G(2d,p) levels. The ultimate ZPEs and anharmonic frequencies were obtained by combining the B3LYP/6-31G(d,p) and B3LYP/6-311+G(2d,p) harmonic values with the B3LYP/6-31+G(d) anharmonic corrections. The Møller−Plesset second-order perturbation optimizations at the MP2(FC)/6-311+G(2d,p) level provided a benchmark energy ordering of the conformers. The Gaussian03[34] program package was used for all DFT and MP2 calculations. The GAMESS program package[35] was used to perform internal coordinate analysis (ICA), whereby the normal mode vibrations are decomposed into linear combinations of internal coordinates deformations (bond stretchings, angle and torsion angle bendings).[36] For a total consistency, ICA was performed after having recalculated the conformers' geometry and frequencies in GAMESS.

In calculating excitation energies, we reoptimized the four conformers at the CASSCF/cc-pVDZ level, using the active spaces of eight electrons distributed among the eight active orbitals, which spanned a feasible configuration space of dimension 1764. The (8,8) active space effectively encompassed all of the chromophores of interest for describing a few lowest excited states in the NAPA conformers. Four of the active orbitals (bonding and the matching antibonding interactions) were localized chiefly in the region of the carbonyl part of the amide and acetyl functional groups, whereas the remaining four originate from the benzene degenerate e_{1g} and e_{2u} highest occupied (HOMO) and lowest unoccupied (LUMO) molecular orbitals. In the CASSCF(8,8) optimized geometries, we next performed the state-averaged CASSCF (SA-CASSCF) calculations over the four lowest equally weighted CASSCF roots. Additionally, SA-CASSCF optimizations of the second root geometries were performed to enable approximation of the adiabatic $S_1 \leftarrow S_0$ excitation energies. The electronic energies of the CASSCF roots were corrected for the dynamic electron correlation via the multistate (MS-CASPT2) method,[37] with the core 1s orbitals on the C, N, and O atoms kept frozen. The imaginary level shift (ILS)[38] parameter of 0.10 au efficiently solved the problems due to intruders, emerging mostly in the first and the third excited state. Upon application of ILS, the reference weights in the excited states approached to within 7% of that in the ground state (around 0.60). To mitigate the problems of overestimating the stability of open shells in CASPT2, the IPEA level shift[39] of 0.10 au was used. The reasons for adopting the reduced value of the IPEA shift parameter (the recommended one is 0.25 au) are discussed elsewhere.[40] The oscillator strengths *f* were calculated from the CASSCF transition dipole moments (TDMs) in the length representation and the MS-CASPT2 energy differences according to

$$f = \frac{2}{3}(\mathrm{TDM})^2 \Delta E \qquad (5)$$

The MOLCAS program package, version 6.4, was used for the multireference calculations.[41]

The 15 lowest TD-DFT excitation energies were computed at the B3LYP/6-31+G(d) optimized geometries of the four conformers. A number of generalized gradient (GGA) and hybrid exchange−correlation functionals were tested preliminarily by their performance on the B_{2u} and B_{1u} excited states of the sole benzene. The present results are based upon the OLYP functional, which combines Handy's recent OPTX modification[42] of the Becke 1988 exchange functional with the Lee−Yang−Parr (LYP) gradient-corrected correlation.[43] We used an extensive Slater-type orbital basis set of TZ2P quality on the O, C, and N atoms and DZP quality on hydrogens, which resulted in 460 symmetrized fragment orbitals. The ADF 2006.01 program package[44] was used for the TD-DFT calculations.[45]

TABLE 1: Geometric Parameters from Figure 2 at Various Levels

conf	level[a]	r_{CO} (Å)	r_{CN1} (Å)	r_{CN2} (Å)	r_{CC1} (Å)	r_{CC2} (Å)	r_{CC3} (Å)	r_{Hb} (Å)	χ[b] (deg)
β(a)	A	1.233	1.363	1.450	1.519	1.537	1.562		−165.5
	B	1.230	1.361	1.446	1.519	1.538	1.563		−155.5
	C	1.225	1.359	1.447	1.515	1.534	1.558		−165.6
	D	1.231	1.359	1.441	1.511	1.523	1.546		−172.1
γ_L(g+)	A	1.238	1.359	1.464	1.517	1.555	1.548	2.001	43.3
	B	1.235	1.357	1.462	1.518	1.555	1.546	1.967	43.0
	C	1.230	1.355	1.461	1.513	1.552	1.543	1.998	43.0
	D	1.236	1.355	1.454	1.510	1.541	1.535	1.986	43.8
γ_L(g−)	A	1.237	1.361	1.467	1.516	1.553	1.538	2.033	−56.0
	B	1.234	1.359	1.466	1.517	1.553	1.537	1.988	−54.0
	C	1.229	1.357	1.464	1.513	1.550	1.533	2.032	−56.3
	D	1.234	1.358	1.457	1.509	1.537	1.526	2.016	−52.8
γ_L(a)	A	1.235	1.364	1.468	1.517	1.550	1.539	2.156	−164.7
	B	1.233	1.362	1.467	1.518	1.551	1.537	2.069	−163.7
	C	1.227	1.360	1.465	1.513	1.547	1.534	2.157	−164.8
	D	1.233	1.362	1.457	1.510	1.535	1.523	2.151	−170.1

[a] A, B3LYP/6-31+G(d); B, B3LYP/6-31G(d,p); C, B3LYP/6-311+G(2d,p); D, MP2/6-311+G(2d,p). [b] Torsion angle χ, N−C_α−C_β−C_γ.

TABLE 2: Electronic Energies and Harmonic and Total (Anharmonic) Zero-Point Energies of the Four NAPA Conformers at Various Levels[a]

	A			B			C			D	E
conf	E	E_{ZPH}	E_{ZPT}	E	E_{ZPH}	E_{ZPT}	E	E_{ZPH}	E_{ZPT}	E	E
β(a)	0.00	0.00	0.00	0.78	0.37	0.67	0.00	0.00	0.00	0.06	0.56
γ_L(g+)	0.17	0.71	0.41	0.00	0.00	0.00	0.28	0.71	0.41	0.00	0.00
γ_L(g−)	0.35	0.56	0.34	1.09	0.74	0.82	0.41	0.60	0.38	1.00	0.57
γ_L(a)	0.49	0.76	0.60	0.94	0.80	0.94	0.52	0.79	0.63	1.26	0.64

[a] E, electronic energy; E_{ZPH}, harmonic zero-point energy; E_{ZPT}, total (anharmonic) zero-point energy. In each column the energies are given in kilocalories per mole, relative to the minimum energy conformer. A, B3LYP/6-31+G(d); B, B3LYP/6-31G(d,p); C, B3LYP/6-311+G(2d,p); D, MP2/6-311+G(2d,p); E, CASSCF(8,8)/MS-CASPT2/cc-pVDZ.

Results and Discussion

A. Geometries and Relative Stability. The most relevant geometric parameters of the four dominant NAPA conformers calculated at the DFT B3LYP/6-31+G(d), B3LYP/6-31G(d,p), and B3LYP/6-311+G(2d,p) levels, as well as the MP2/6-311+G(2d,p) level, are collected in Table 1. Table 2 confronts several theoretical models as to their predictions on the relative stabilities of the conformers, at first only with respect to the electronic energies and then upon inclusion of the harmonic and anharmonic vibrational corrections.

For the most part, B3LYP with different basis sets and MP2 exhibit relatively small differences in the bond lengths of the peptide backbone, with the majority of them remaining within 0.01 Å. A peculiar noteworthy disagreement is found between B3LYP/6-31+G(d) and B3LYP/6-31G(d,p) in the position of the side chain of the β(a) conformer, where the two χ(N−C_α−C_β−C_γ) torsion angles differ by ∼10° (Table 1). Increasing the flexibility of the valence shell and extending the basis set with additional sets of polarization functions [6-311+G(2d,p)] generally leads to a slight contraction of the bonds.

Whereas the peptide backbone remains essentially unaffected, the treatment of the hydrogen-bonding interactions is critically dependent upon both the method and the basis set. These subtle effects are capable of changing the energy ordering of the conformers. Thus, if only electronic energies are considered, the extended β(a) structure is the most stable structure via B3LYP/6-31+G(d) and B3LYP/6-311+G(2d,p), while B3LYP/6-31G(d,p) and CASSCF(8,8)/MS-CASPT2/cc-pVDZ predict the γ_L(g+) conformer to be the most stable (Table 2). At the MP2/6-311+G(2d,p) level, γ_L(g+) and β(a) are predicted as effectively isoenergetic with an energy difference of only 0.06 kcal mol^{-1} in favor of γ_L(g+). The remaining conformers, however, lie much higher in energy: γ_L(g−) 1.00 kcal mol^{-1} and γ_L(a) 1.26 kcal mol^{-1} above γ_L(g+). When we turn to the harmonic ZPE corrections (ZPE_H), B3LYP predicts larger ZPE_H for γ_L(g+) than for β(a), effectively destabilizing the former by 0.54, 0.41, and 0.43 kcal mol^{-1} at the 6-31+G(d), 6-31G(d,p) and 6-311+G(2d,p) levels, respectively. Because of the size of the system and the large computational effort needed for the calculation of anharmonic corrections, these were computed only with the 6-31+G(d) basis set and combined with the harmonic frequencies from all three levels. Our computations reveal corrections of −2.01, −1.92, −1.86, and −1.70 kcal mol^{-1} for γ_L(g+), γ_L(a), γ_L(g−), and β(a), respectively. Hence the anharmonic correction stabilizes γ_L(g+).

The B3LYP r_{Hb} distances change by 0.034 Å in γ_L(g+), 0.045 Å in γ_L(g−), and 0.087 Å in γ_L(a) upon moving from 6-31+G(d) to 6-31G(d,p). With the MP2/6-311+G(2d,p) results taken as a reference, it transpires that hydrogen bonding is most likely underestimated by the former and overestimated by the latter basis set. The introduction of diffuse functions on the second-row atoms fixes the r_{Hb} distances above 2 Å in all cases, regardless of the presence of additional sets of polarization functions. It is known, however, that diffuse functions become important primarily in the case of very strong hydrogen bonds, when the donor atom bears a highly anionic character,[46] or in studying proton transfer,[14] when geometries far from equilibria are involved. Extending the basis set with the p-type functions on the H atoms appears more relevant for the present case and leads to a better description of the N−H and C−H stretches, and hence more reliable ZPEs.

The intramolecular basis-set superposition error (BSSE) is yet another issue worth checking when delicate energy differences govern the relative stability of the conformers. This effect was probed for the B3LYP/6-31+G(d) and B3LYP/6-31G(d,p) levels for the most competitive β(a) and γ_L(g+) conformers

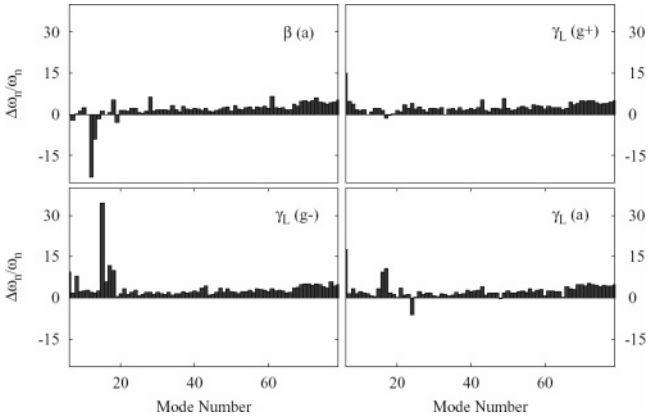

Figure 3. B3LYP/6-31+G(d) anharmonic contributions to the normal mode vibrations in the four NAPA conformers.

according to the counterpoise procedure proposed by Jensen.[47] The basis set of β(a) was supplemented with the ghost functions located at the atoms of γ_L(g+) (excluding only the atoms of the largely unchanged Phe side chain), and conversely for γ_L-(g+). With the 6-31+G(d) basis set, the BSSE correction reduces the difference in electronic energies of β(a) and γ_L-(g+) to only 0.11 kcal mol^{-1}. The intramolecular BSSE is larger with the 6-31G(d,p) basis set, so γ_L(g+) drops further below β(a) by 0.18 kcal mol^{-1} at that level, resulting in a total 0.96 kcal mol^{-1} energy difference in favor of γ_L(g+). On the basis of these calculations, we also estimate that with our largest [6-311+G(2d,p)] basis set the effect of the intramolecular BSSE is reduced to below 0.05 kcal mol^{-1} with the B3LYP functional. As pointed out by van Mourik et al.,[48] the MP2 intramolecular BSSE may be somewhat larger.

Judging from the trends in the bond lengths of the four conformers (Table 1), it can be concluded that the γ_L structures are on one hand stabilized via possibilities of the hydrogen bonding in the C7 ring and the NH$\cdots\pi$ interaction (vide infra) and on the other hand destabilized by increased steric strains. The r_{CC2} and r_{CN2} distances in the γ_L conformers, being elongated by almost 0.02 Å relative to β(a), are most indicative of the steric strains in the C7 ring, which accommodates the large Phe substituent. Because a very delicate balance of the two opposing effects determines the most stable conformation, it is difficult to draw definite conclusions on the conformational preferences of NAPA. Our results cast doubts on the energy sequence from the B3LYP/6-31+G(d) level,[6] which indicates propensity toward the extended β(a)-like structures. An additional insight into the interactions that lead to stabilization of a specific conformer is needed and will be sought in the analysis of the IR signature of different backbone foldings.

B. Vibrational Analysis. Figure 3 displays the B3LYP/6-31+G(d) anharmonic contributions to the normal mode vibrations, expressed as the ratio of the difference between the harmonic and anharmonic frequency ($\Delta_i = \omega_i - \nu_i$) to the harmonic frequency ω_i of a given mode.

The low-frequency modes (below 100 cm^{-1}) are omitted because of the expected errors in the numerical treatment of very shallow potentials.

From Figure 3 it is apparent that the stabilization of the γ_L conformers arises from a general red shift in all vibrational modes. For stabilizing interactions, apart from the hydrogen bonding in the C5 and C7 rings, one can also expect the NH$\cdots\pi$ interaction (N of the peptide bond) in γ_L and NH$_2\cdots\pi$ (N of the amide residue) in the β(a) conformer. In particular, the NH-(Phe) out-of-plane bending mode of γ_L(g−) at 450 cm^{-1}, which undergoes red-shifting by 156 cm^{-1}, strongly promotes the NH$\cdots\pi$ interaction. Likewise, in γ_L(g+), the in-plane NH(Phe) bending mode at 1114 cm^{-1} and the NH$_2$ in-plane bending at 1303 cm^{-1} undergo red-shifting by 61 and 74 cm^{-1}, respectively. On the contrary, the C5 structure of β(a) requires a rigid backbone involving only a limited interaction with the aromatic side chain. In fact, the out-of-plane NH$_2$ bending mode is suppressing the NH$_2\cdots\pi$ interaction and its anharmonic frequency is blue-shifted by 15 cm^{-1} compared to the harmonic value.

TABLE 3: Vibrational Analysis of the Amide A Band at the B3LYP/6-31+G(d) Level[a]

	NH(Phe)			NH_2^{sym}			NH_2^{asym}		
conf	ω	ν	w^{exp}	ω	ν	w^{exp}	ω	ν	w^{exp}
β(a)	3575	3391	3434	3569	3408	3426	3694	3512	3543
γ_L(g+)	3587	3411	3438	3482	3324	3342	3663	3476	3516
γ_L(g−)	3615	3436		3487	3335	3348	3658	3481	3517
γ_L(a)	3610	3440		3513	3358		3659	3476	

[a] Harmonic (ω), anharmonic (ν), and experimental (ω^{exp}) frequencies[6] (given in reciprocal centimeters) of NH(Phe) and symmetric and antisymmetric NH$_2$ stretches are compared.

The presence of the two amide groups in the system gives rise to three components of the amide A band: the phenylalanine NH stretch [denoted NH(Phe)], and the symmetric and antisymmetric stretches of the terminal NH$_2$ group. The strength of the interactions that involve the amide groups can be estimated from the frequency shift of the amide modes relative to the frequency of the free amide group occurring in the 3420−3550 cm^{-1} region, as well as from the splitting between the symmetric and the antisymmetric NH$_2$ modes.[49] In Table 3 we confront the harmonic and anharmonic frequencies of the amide A band of the four NAPA conformers at the B3LYP/6-31+G-(d) level and the available experimental frequencies.[6] Inspection of Table 3 immediately reveals a notable discrepancy between the anharmonically corrected and experimental frequencies. The former are systematically red-shifted by 30−40 cm^{-1} compared to the expected values, which indicates deficiencies of the B3LYP/6-31+G(d) harmonic spectrum.

It should be noted that the amide A frequencies are not sufficient to distinguish unambiguously between the γ_L(g−) and γ_L(a) conformers, so that the experimental assignment was assisted by the amide I frequencies. A much better agreement with experimental amide A vibrations is found for the anharmonic B3LYP/6-31G(d,p) frequencies, as indicated in Table 4. These have been obtained by adding the B3LYP/6-31+G(d) anharmonic corrections for the amide A modes to the corresponding harmonic B3LYP/6-31G(d,p) frequencies. The only exception is found for the NH(Phe) stretch of the β(a) conformer and will be explained shortly. Table 4 also compiles the harmonic and anharmonic B3LYP/6-311+G(2d,p) frequencies, but as expected from the corresponding geometries, these do not provide an improvement over the B3LYP/6-31+G(d) ones.

Focusing on the B3LYP/6-31G(d,p) results, one notices that in β(a) both NH$_2$ stretches are shifted toward higher frequencies than in the remaining conformers. The high frequency of these stretches indicates that the terminal NH$_2$ group is not involved in H-bonding interactions. This is apparent also from the N−H bond lengths, which are negligibly changed. The difference of 118 cm^{-1} in frequencies of the two stretches is very close to the 116 cm^{-1} splitting typical of the free NH$_2$ group and is in excellent agreement with the experimental value of 117 cm^{-1}. The almost "free" NH$_2$ splitting is a direct indication of the very weak coupling between the amide hydrogen and the phenyl π-electronic system. This contrasts the situation in the γ_L

TABLE 4: Vibrational Analysis of the Amide A Band[a]

	B3LYP/6-31G(d,p)						B3LYP/6-311+G(2d,p)					
	NH(Phe)		NH_2^{sym}		NH_2^{asym}		NH(Phe)		NH_2^{sym}		NH_2^{asym}	
conf	ω	ν	ω	ν	ω	ν	ω	ν	ω	ν	ω	ν
β(a)	3587	3403	3582	3421	3721	3539	3584	3400	3569	3408	3695	3513
γ_L(g+)	3610	3434	3479	3321	3655	3504	3596	3420	3476	3318	3667	3480
γ_L(g−)	3639	3460	3485	3333	3643	3506	3626	3447	3482	3330	3659	3482
γ_L(a)	3638	3468	3507	3352	3644	3509	3622	3452	3511	3356	3660	3477

[a] Harmonic (ω) and anharmonic (ν) frequencies (given in reciprocal centimeters) of NH(Phe) and symmetric and antisymmetric NH_2 stretches are compared.

TABLE 5: Harmonic and Anharmonic Frequencies and Potential Energy Distribution[a] of the Amide I Band

		Harmonic (ω) and Anharmonic (ν) Frequencies (cm^{-1})							
		amide $I^{(1)}$				amide $I^{(2)}$			
conf	level[b]	ω	int[c]	ν	PED	ω	int[c]	ν	PED
β(a)	A	1729	355	1698	$CO^{(1)}$ s (0.76), $CO^{(2)}$ s (0.05), CCH d (0.04),	1760	269	1732	$CO^{(2)}$ s (0.7), $CN^{(2)}$ s (0.08), $NH_2^{(2)}$ ib (0.07),
	B	1755	265	724	CNH ib (0.04), CN s (0.03)	1790	238	1762	$CCN^{(2)}$ s (0.04), $CO^{(1)}$ s (0.04)
	C	1711	349	1680		1741	258	1713	
γ_L(g+)	A	1719	211	1688	$CO^{(1)}$ s (0.72), CN s (0.07),	1761	408	1721	$CO^{(2)}$ s (0.77), $CN^{(2)}$ s (0.09),
	B	1742	179	1711	NH_2 ib (0.07), CCN d (0.05)	1788	348	1748	CNH ib (0.06), $CCN^{(2)}$ s (0.04)
	C	1700	204	1669		1741	401	1701	
γ_L(g−)	A	1721	188	1691	$CO^{(1)}$ s (0.74), CN s (0.07), NH_2 ib (0.06),	1769	418	1733	$CO^{(2)}$ s (0.76), $CN^{(2)}$ s (0.09), $NH_2^{(2)}$ ib (0.06),
	B	1746	166	1716	CNH d (0.06), NCC d (0.04)	1803	328	1767	CNH ib (0.06), $CCN^{(2)}$ s (0.04)
	C	1702	185	1672		1752	409	1716	
γ_L(a)	A	1723	183	1720	$CO^{(1)}$ s (0.74), CNH ib (0.06),	1770	379	1699	$CO^{(2)}$ s (0.76), $CN^{(2)}$ s (0.09), $NH_2^{(2)}$ ib (0.06),
	B	1748	150	1725	CCN d (0.04), CN s (0.03)	1797	322	1747	CNH ib (0.06), $CCN^{(2)}$ s (0.04)
	C	1705	180	1702		1752	367	1681	

[a] s = stretching, ib = in-plane bending, d = deformation. [b] A, B3LYP/6-31+G(d); B, B3LYP/6-31G(d,p); C, B3LYP/6-311+G(2d,p). [c] The given IR intensities (kilometers per mole) are for the harmonic transitions.

conformers, where the terminal NH_2 group participates in an H-bonded C7 ring, and both NH_2 stretches are found at lower frequencies. The asymmetric stretch is regularly found between 3504− and 3509 cm^{-1} and the symmetric stretch between 3321− and 3352 cm^{-1}. Accordingly, the splitting between the two components is larger than in β(a), equalling 182, 173, and 147 cm^{-1} in the γ_L(g+), γ_L(g−), and γ_L(a) conformers, respectively. The first two values are very close to the experimental splittings of 174 and 169 cm^{-1} assigned to γ_L(g+) and γ_L(g−), respectively.[6]

In the γ_L conformers, the NH(Phe) stretch is intercalated between the two NH_2 stretches. The strength of the interaction between the N−H bond and the phenyl ring can be monitored by the softening of the NH(Phe) bond. The most red-shifted NH(Phe) frequency at 3411 cm^{-1} is found for γ_L(g+), suggesting the strongest interaction with the side chain. Because of the close contact with the CO group of the same residue, the NH(Phe) stretch of β(a) is found at 3403 cm^{-1}, which is approximately 30 cm^{-1} lower than the experimental frequency of 3434 cm^{-1}. The reason is that the NH(Phe) and the symmetric NH_2 stretch participate in a Fermi type I resonance interaction that was not recognized by the perturbative anharmonic analysis. In other words, the NH−C_α−CO interaction appears overestimated by the anharmonic treatment, and once the Fermi resonance is taken into account it is expected to further destabilize the β(a) structure.

Let us now investigate some features of the NAPA conformers that are not directly related to UV/IR experiments. The amide I band, as the most intense, has been used extensively in the identification of secondary structures.[50] It arises mainly from the CO stretching vibrations. The two carbonyl groups of NAPA give rise to two amide I modes, denoted as amide $I^{(1)}$ and amide $I^{(2)}$, as shown in Figure 1. The amide I frequencies are summarized in Table 5. Unfortunately, experimental amide I frequencies of NAPA are not available for comparison.

Inspection of the amide $I^{(1)}$ modes reveals separation into two subgroups. The γ_L(g+) and γ_L(g−) conformers form a medium-strong H-bonded C7 ring with r_{Hb} distances of 1.986 and 2.016 Å computed at the MP2/6-311+G(2d,p) level. For these conformers the amide $I^{(1)}$ anharmonic B3LYP/6-31G(d,p) frequencies are found at 1711 and 1716 cm^{-1}, respectively. The γ_L(a) structure experiences a much weaker H-bond with r_{Hb} = 2.151 Å, while in the β(a) structure the $CO^{(1)}$ group is H-bond-free. Consequently, the amide $I^{(1)}$ modes of these conformers are less anharmonic, equalling 1725 and 1724 cm^{-1}, respectively.

By analogy to the amide A vibrations, the splitting of the two amide I components provides information on the differences between the environments of the two CO groups. The highest amide $I^{(2)}$ frequency of 1762 cm^{-1} corresponds to the unhindered $CO^{(2)}$ group of the γ_L(g−) structure, which also exhibits the largest amide I splitting. To test the sensitivity of the splitting between the two amide I modes on the CO environment, we substituted the N-terminal acetyl by a formyl group (i.e., H atom instead of CH_3). This led to an upshift of the harmonic amide $I^{(1)}$ frequencies in all conformers. Specifically, the amide $I^{(1)}$ frequencies computed at the B3LYP/6-31+G(d) level are now found at 1752, 1747, 1748, and 1750 cm^{-1} in β(a), γ_L(g+), γ_L(g−), and γ_L(a), respectively, while the corresponding splittings are reduced to only 15, 28, 27, and 27 cm^{-1}.

The internal coordinate analysis of the amide I modes reveals the character and degree of couplings between the two amide I modes (Table 5). The $CO^{(2)}$ bond of the β(a) structure and the $CO^{(1)}$ of the γ_L structures are engaged in C5 and C7 interactions, respectively. In such cases the CO stretching contribution to the amide I vibration is between 70%− and 74% depending on the strength of the ring-forming interaction. Meanwhile, the

TABLE 6: Vertical (T_v) and Adiabatic (T_0) Excitation Energies (eV) and Oscillator Strengths (Length Representation $\times$ 10^2 in Parentheses) of the Four NAPA Conformers at the (A) CASSCF(8,8)/MS-CASPT2/cc-pVDZ and (B) TD-OLYP/TZ2P(DZP) Levels

	β(a)				γ_L(g+)			
	A		B		A		B	
state	T_v	T_0	T_v	exp[6]	T_v	T_0	T_v	exp[6]
1	4.827 (0.25)	4.707	5.133 (0.64)	4.650	4.882 (0.34)	4.769	5.113 (0.12)	4.663
2	5.946 (5.00)				6.012 (7.35)			
3	6.809 (88.5)				6.973 (86.8)			

	γ_L(g−)			γ_L(a)			
	A			A		B	
state	T_v	T_0	T_v	T_v	T_0	T_v	exp[6]
1	4.913 (0.40)	4.778	5.125 (0.18)	4.854 (0.38)	4.777	5.113 (0.23)	4.654
2	6.040 (9.02)			5.986 (7.00)			
3	6.972 (86.2)			6.967 (83.3)			

H-bond-free CO groups contribute more to the amide I vibration, around 76−77%. These values can be compared to those obtained by DeFlores et al.[30] for *N*-methylacetamide (one peptide unit), where a larger CO stretching contribution of 81% was found. Obviously, H-bonding promotes delocalization of the amide I vibration within the C7 ring, reducing the contribution of the CO atomic displacements within the vibration. This can be deduced from the significant contribution of NH_2 in-plane bending and CCN deformation in the amide $I^{(1)}$ vibration of both the γ_L(g+) and γ_L(g−) conformers. Also, an important message of Table 5 is the lower IR intensities of amide I vibrations belonging to CO groups that are engaged in H-bonding compared to the "free" CO groups, which is in accordance with the perturbational treatment of Miyazawa.[51] Finally, direct evidence of couplings between the two amide I bands is found only in the extended β(a) structure, where the contribution of the neighboring CO stretch amounts to 4−5%.

C. Excited States. Excitation energies and oscillator strengths in the length representation corresponding to a few lowest transitions in the four NAPA conformers are shown in Table 6. While the multistate CASPT2 energies are used in calculating the excitation energies, the differences between the single- and multi-state CASPT2 values are very small, in all cases less than 0.02 eV. This is a consequence of the reference CASPT2 states nicely dominating the resulting MS-CASPT2 states, typically by more than 99%.

On the basis of the analysis of active occupancies in the SA-CASSCF reference wave functions, the three lowest transitions in NAPA correspond predominantly to local excitations in the Phe chromophore. These can be considered as closely analogous to the much-studied $^1B_{2u} \leftarrow \tilde{X}$, $^1B_{1u} \leftarrow \tilde{X}$, and $^1E_{1u} \leftarrow \tilde{X}$ transitions in benzene,[52] which derive from a single LUMO ← HOMO ($e_{2u} \leftarrow e_{1g}$) excitation and whose experimental band maxima are located at 4.90, 6.20, and 6.94 eV, respectively.[53,54] Owing to the fact that $^1B_{2u} \leftarrow \tilde{X}$ and $^1B_{1u} \leftarrow \tilde{X}$ are symmetry-forbidden in benzene, whereas $^1E_{1u} \leftarrow \tilde{X}$ is allowed, the first two transitions in NAPA have much weaker intensities than the third one, as is expected (Table 6). To get a better idea of the accuracy of the present CASSCF-CASPT2/cc-pVDZ approach, calculations on the $^1B_{2u}$, $^1B_{1u}$, and $^1E_{1u}$ states of benzene were performed with the same IPEA and imaginary level shifts as in NAPA (0.10 au), and a (6,6) π-active space. This resulted in 4.97, 6.47, and 7.06 eV vertical excitation energies, respectively, which is reasonable in view of the known mismatches between the vertical excitation energies and observed band maxima in benzene.[52]

In the NAPA conformers all three excitation energies are red-shifted relative to benzene, most notably the second excited state, which is lowered by ∼0.5 eV compared to the parent $^1B_{1u} \leftarrow \tilde{X}$ transition (Table 6). Such differences are indicative of the Phe chromophore interactions with the peptide backbone. For instance, the calculated higher $S_1 \leftarrow S_0$ vertical excitation energies, such as in γ_L(g+) and γ_L(g−), presumably reflect the stabilization of the Phe chromophore "HOMO" via the NH···π interaction (vide ante).

Three band systems were distinguished in the R2PI spectrum of NAPA.[6] On the basis of vibrational progressions, the lowest-lying system was assigned to the β(a) conformer.[6] This is supported by the CASSCF/MS-CASPT2 calculations, although a mismatch of ∼0.18 eV is present, which is, however, still within the error bounds of the method (0.20 eV).[27] To a certain extent the absolute accuracy of the present multireference approach suffers from the relatively small basis set but also from the fact that a more detailed analysis of the spectrum, for example, inclusion of the vibronic coupling, is practically impossible. It was stressed that calculated vertical excitation energies of the symmetry-forbidden transitions (or transitions originating from these, as is the case with NAPA) are not straightforwardly compared to the observed band maxima.[52] The calculated adiabatic excitation energies approach the experimental band maxima more closely (within 0.12 eV, Table 6), albeit the ordering of the conformers' adiabatic transitions differs from the vertical ones, which suggests complex overlapping of the band systems. Another issue is predicted larger differences in the $S_1 \leftarrow S_0$ excitation energies between different conformers than what is observed in the R2PI spectrum (Table 6). Thus the second lowest conformer is calculated as blue-shifted by 0.028 eV relative to β(a), while it is observed only 0.004 eV higher, at 4.654 eV. This peak was tentatively associated with either γ_L(g−) or γ_L(a),[6] but the calculations unambiguously point toward γ_L(a), whose vertical transition should be well resolved from γ_L(g−). The γ_L(g+) conformer correctly appears as the third peak but again as too blue-shifted (0.055 eV) from β(a) compared to the experimental value of 0.013 eV. According to CASSCF/MS-CASPT2, there might be present a fourth spectral system belonging to γ_L(g−), which is further blue-shifted from γ_L(g+) by ∼0.03 eV.

By far the most intense peaks in the R2PI spectrum correspond to β(a), followed by γ_L(g+).[6] Here the theoretical approach deviates most notably, because the vertical oscillator strength of β(a) is even predicted to be the smallest of the four conformers (Table 6). While this may partly be the issue with the uncorrelated CASSCF transition dipole moments, the spectral intensity also depends upon the relative population of the conformers in the S_0 state. Energetically this should favor β(a) and γ_L(g+), although only mildly, and it remains difficult to account for the observed large differences in intensities. Consequently, entropic and kinetic factors might play a prominent role in the final relative distribution of the conformers under experimental conditions.

Numerous low-lying transitions in the ∼4.2−6.0 eV region result via the TD-OLYP approach. The vast majority of them correspond to the intramolecular charge transfers (CT)[55] from the distant carbonyl bonds to the antibonding orbitals of the Phe chromophore. It is well-known that such CT states tend to

be grossly underestimated by TD-DFT,[56] appearing roughly as differences in the Kohn−Sham eigenvalues of the orbitals involved, which is precisely the situation with NAPA. Thus, regardless of the GGA functional used, 14 of the 15 lowest TD-DFT excited states are of the similar CT type invariably appearing in quasidegenerate pairs, which reflects quasidegeneracies of the antibonding orbitals of the Phe chromophore. These low-lying CT states must be considered illusive, knowing that the CASSCF active space comprises all of the orbitals necessary for describing them and that they are still absent from the CASSCF/MS-CASPT2 spectrum in the 4.8−7.0 eV region. The only state principally involving localized excitations within the Phe chromophore is found much higher in the TD-OLYP spectra, around 5.1 eV (Table 6). This state is satisfactorily decoupled from the erroneously described charge-transfer configurations and is as such best compared to the experimental $S_1 \leftarrow S_0$ transitions. However, apart from the large absolute differences between the TD-OLYP values and the experiment, the predicted spectral sequence of the conformers matches neither CASSCF/MS-CASPT2 nor the experimental assignments. In addition, resorting to the popular hybrid functionals (B3LYP, BP86) did not prove beneficial. For these reasons we conclude that present TD-DFT functionals are highly unreliable for similar systems.

Conclusions

We present a computational study of the conformational preferences of *N*-acetylphenylalaninylamide (NAPA). This model system featuring two peptide units is of general importance because it permits high-quality theoretical investigation of the interactions that shape the peptide backbone while simultaneously allowing for a direct comparison with experimental data. Our analysis focuses on the relative stability and spectroscopic properties of the four most stable NAPA conformers. It relies on high-quality MP2/6-311+G(2d,p) electronic energies, DFT-based second-order perturbative treatment of molecular anharmonicities, and CASSCF/MS-CASPT2 calculations of the excited states.

The first message of this study is the sensitivity of the conformers' relative stability on the level of quantum chemical computations. While experimental assignments have been based almost exclusively on the combination of the B3LYP functional and the 6-31+G(d) basis set,[6] we have shown that the relative stability of conformers as deduced from this level might be erroneous. Compared to the reference MP2/6-311+G(2d,p) level, B3LYP/6-31+G(d) significantly underestimates hydrogen-bonding interactions. Summarizing three aspects—the relative stability of γ_L(g+) with respect to β(a) obtained by the extensive MP2 computations, the largest splitting between the symmetric and antisymmetric NH_2 stretches encountered in γ_L(g+) (reflecting the strength of the C7 H-bonding interaction), and finally the softness of the respective NH(Phe) bond—we believe that the extended β(a) form might not represent the lowest energy conformer of NAPA.

The assigned sequence, by which the $S_1 \leftarrow S_0$ transitions of the NAPA conformers appear in the spectrum, is well supported by the vertical CASSCF/MS-CASPT2 excitation energies. In contrast, the excited states obtained via TD-DFT appear highly unreliable, which effectively proves TD-DFT unsuitable for the present systems.

Acknowledgment. We acknowledge the financial support of the Croatian Ministry of Science and Technology under Projects 098-0352851-2921 and 098-0982915-2944. Part of the calculations were performed on the Isabella cluster at the University of Zagreb Computing Center (SRCE).

References and Notes

(1) Robertson, E. G.; Simons, J. P. *Phys. Chem. Chem. Phys.* **2001**, *3*, 1.
(2) Snoek, L. C.; Kroemer, R. T.; Hockridge, M. R.; Simons, J. P. *Phys. Chem. Chem. Phys*. **2001**, *3*, 1819.
(3) Dian, B. C.; Longarte, A.; Mercier, S.; Evans, D. A.; Wales, D. J.; Zwier, T. S. *J. Chem. Phys*. **2002**, *117*, 10688.
(4) Hünig, I.; Kleinermanns, K. *Phys. Chem. Chem. Phys.* **2004**, *6*, 2650.
(5) Bakker, J. M.; Plützer, C.; Hünig, I.; Häber, T.; Compagnon, I.; von Helden, G.; Meijer, G.; Kleinermanns, K. *ChemPhysChem.* **2005**, *6*, 120.
(6) Chin, W.; Mons, M.; Dognon, J.-P.; Piuzzi, F.; Tardivel, B.; Dimicoli, I. *Phys. Chem. Chem. Phys.* **2004**, *6*, 2700.
(7) Chin, W.; Piuzzi, F.; Dimicoli, I.; Mons, M. *Phys. Chem. Chem. Phys.* **2006**, *8*, 1033.
(8) Chin, W.; Dognon, J.-P.; Canuel, C.; Piuzzi, F.; Dimicoli, I.; Mons, M.; Compagnon, I.; von Helden, G.; Meijer, G. *J. Chem. Phys.* **2005**, *122*, 054317.
(9) Chin, W.; Compagnon, I.; Dognon, J.-P.; Canuel, C.; Piuzzi, F.; Dimicoli, I.; von Helden, G.; Meijer, G.; Mons, M. *J. Am. Chem. Soc.* **2005**, *127*, 1388.
(10) Scott, A. P.; Radom, L. *J. Phys. Chem.* **1996**, *100*, 16502.
(11) Dian, B. C.; Longarte, A.; Zwier, T. S. *Science* **2002**, *296*, 2369.
(12) Došlić, N.; Kühn, O. *Z. Phys. Chem.* **2003**, *217*, 1507.
(13) Antony, J.; van Helden, G.; Meijer, G.; Schmidt, B. *J. Chem. Phys.* **2005**, *123*, 014305.
(14) Matanović, I.; Došlić, N. *J. Phys. Chem. A* **2005**, *109*, 4185.
(15) van Mourik, T.; Benoit, D. M.; Price, S. L.; Clary, D. C. *Phys. Chem. Chem. Phys.* **2000**, *2*, 1281.
(16) Gerber, R. B.; Jung, J. O. *Computational Molecular Spectroscopy*; Jensen, P., Bunker, P. R., Eds.; John Wiley: New York, 2000; p 365.
(17) Gregurick, S. K.; Fredj, E.; Elber, R.; Gerber, R. B. *J. Phys. Chem. B* **1997**, *101*, 8595.
(18) Roitberg, A. E.; Gerber, R. B.; Elber, R.; Ratner, M. A. *Science* **1995**, *268*, 1319.
(19) Gerber, R. B.; Brauer, B.; Gregurick, S. K.; Chaban, G. M. *Phys. Chem. Chem. Phys.* **2002**, *5*, 142.
(20) Barone, V. *J. Chem. Phys.* **2004**, *120*, 3059.
(21) Barone, V. *J. Chem. Phys.* **2005**, *122*, 014108.
(22) Matanović, I.; Došlić, N. *Int. J. Quantum Chem.* **2006**, *106*, 1367.
(23) Kovačević, G.; Hrenar, T.; Došlić, N. *Chem. Phys.* **2003**, *293*, 41.
(24) Roos, B. O.; Taylor, P. R.; Siegbahn, P. E. M. *Chem. Phys.* **1980**, *48*, 157.
(25) Andersson, K.; Malmqvist, P.-Å.; Roos, B. O. *J. Chem. Phys*. **1992**, *96*, 1218.
(26) Runge, E.; Gross, E. K. U. *Phys. Rev. Lett.* **1984**, *52*, 997.
(27) Roos, B. O.; Andersson, K.; Fülscher, M. P.; Serrano-Andrés, L.; Pierloot, K.; Merchán, M.; Molina, V. *J. Mol. Struct. (THEOCHEM)* **1996**, *388*, 257.
(28) Tozer, D. J.; Amos, R. D.; Handy, N. C.; Roos, B. O.; Serrano-Andrés, L. *Mol. Phys.* **1999**, *97*, 859.
(29) Branden, C.; Tooze, J. *Introduction to Protein Structure*; Garland: New York, 1991.
(30) DeFlores, L. P.; Ganim, Z.; Ackley, S. F.; Chung, H. S.; Tokmakoff, A. *J. Phys. Chem. B* **2006**, *110*, 18973.
(31) Kollman, P.; Dixon, R.; Cornell, W.; Fox, T.; Chipot, C.; Pohirille, A. *Computer Simulation of Biomolecular Systems: Theoretical and Experimental Applications*; van Gusteren, W. F., Weiner, P. K., Wilkinson, A. J., Eds.; ESCOM: Leiden, The Netherlands, 1997; p 83.
(32) Ponder, J. W. *TINKER: Software Tools for Molecular Design*, 4.1 ed.; Washington University School of Medicine: St. Louis, MO, 2003.
(33) Becke, A. D. *J. Chem. Phys.* **1993**, *98*, 5648.
(34) Frisch, M. J.; Trucks, G. W.; Schlegel, H. B.; Scuseria, G. E.; Robb, M. A.; Cheeseman, J. R.; Montgomery, J. A., Jr.; Vreven, T.; Kudin, K. N.; Burant, J. C.; Millam, J. M.; Iyengar, S. S.; Tomasi, J.; Barone, V.; Mennucci, B.; Cossi, M.; Scalmani, G.; Rega, N.; Petersson, G. A.; Nakatsuji, H.; Hada, M.; Ehara, M.; Toyota, K.; Fukuda, R.; Hasegawa, J.; Ishida, M.; Nakajima, T.; Honda, Y.; Kitao, O.; Nakai, H.; Klene, M.; Li, X.; Knox, J. E.; Hratchian, H. P.; Cross, J. B.; Bakken, V.; Adamo, C.; Jaramillo, J.; Gomperts, R.; Stratmann, R. E.; Yazyev, O.; Austin, A. J.; Cammi, R.; Pomelli, C.; Ochterski, J. W.; Ayala, P. Y.; Morokuma, K.; Voth, G. A.; Salvador, P.; Dannenberg, J. J.; Zakrzewski, V. G.; Dapprich, S.; Daniels, A. D.; Strain, M. C.; Farkas, O.; Malick, D. K.; Rabuck, A. D.; Raghavachari, K.; Foresman, J. B.; Ortiz, J. V.; Cui, Q.; Baboul, A. G.; Clifford, S.; Cioslowski, J.; Stefanov, B. B.; Liu, G.; Liashenko, A.; Piskorz, P.; Komaromi, I.; Martin, R. L.; Fox, D. J.; Keith, T.; Al-Laham, M. A.; Peng, C. Y.; Nanayakkara, A.; Challacombe, M.; Gill, P. M. W.;

Johnson, B.; Chen, W.; Wong, M. W.; Gonzalez, C.; Pople, J. A. *Gaussian 03*, Revision C.02; Gaussian, Inc.: Wallingford, CT, 2004.

(35) Schmidt, M. W.; Baldridge, K. K.; Boatz, J. A.; Elbert, S. T.; Gordon, M. S.; Jensen, J. H.; Koseki, S.; Matsunaga, N.; Nguyen, K. A.; Su, S. J.; Windus, T. L.; Dupuis, M.; Montgomery, J. A. *J. Comput. Chem.* **1993**, *14*, 1347.

(36) Boatz, J. A.; Gordon, M. S. *J. Phys. Chem.* **1989**, *93*, 1819.

(37) Finley, J.; Malmqvist, P.-Å.; Roos, B. O.; Serrano-Andrés, L. *Chem. Phys. Lett.* **1998**, *288*, 299.

(38) Forsberg, N.; Malmqvist, P.-Å. *Chem. Phys. Lett.* **1997**, *274*, 196.

(39) Ghigo, G.; Roos, B. O.; Malmqvist, P.-Å. *Chem. Phys. Lett.* **2004**, *396*, 142.

(40) Ljubić I.; Sabljić, A. *J. Phys. Chem. A* **2007**, *111*, 1339.

(41) Karlström, G.; Lindh, R.; Malmqvist, P.-Å.; Roos, B. O.; Ryde, U.; Veryazov, V.; Widmark, P.-O.; Cossi, M.; Schimmelpfennig, B.; Neogrady, P.; Seijo, L. *Comput. Mater. Sci.* **2003**, *28*, 222.

(42) Handy, N. C.; Cohen, A. J. *Mol. Phys.* **2001**, *99*, 403.

(43) Lee, C.; Yang, W.; Parr, R. G. *Phys. Rev. B* **1988**, *37*, 785.

(44) (a) ADF 2006.01, SCM, Theoretical Chemistry, Vrije Universiteit, Amsterdam, The Netherlands, http://www.scm.com. (b) te Velde, G.; Bickelhaupt, F. M.; van Gisbergen, S. J. A.; Fonseca Guerra, C.; Baerends, E. J.; Snijders, J. G.; Ziegler, T. *J. Comput. Chem.* **2001**, *22*, 931.

(45) van Gisbergen, S. J. A.; Snijders, J. G.; Baerends, E. J. *Comput. Phys. Commun.* **1999**, *118*, 119.

(46) (a) Šponer, J.; Hobza, P. *Chem. Phys. Lett.* **1997**, *267*, 263. (b) Hoffmann, M.; Rychlewski, J. *Comput. Methods Sci. Technol.* **2000**, *6*, 61.

(47) Jensen, F. *Chem. Phys. Lett.* **1996**, *261*, 633.

(48) van Mourik, T.; Karamertzanis, P. G.; Price, S. L. *J. Phys. Chem. A* **2006**, *110*, 8.

(49) Robertson, E. G.; Hockridge, M. R.; Jelfs, P. D.; Simons, J. P. *Phys. Chem. Chem. Phys.* **2001**, *3*, 1819.

(50) Barth, A.; Zscherp, C. *Q. Rev. Biophys.* **2002**, *35*, 369.

(51) Miyazawa, T. *J. Chem. Phys.* **1960**, *32*, 1647.

(52) Bernhardsson, A.; Forsberg, N.; Malmqvist, P.-Å.; Roos, B. O.; Serrano-Andrés, L. *J. Chem. Phys.* **2000**, *112*, 2798.

(53) Hiraya, A.; Shobatake, K. *J. Chem. Phys.* **1991**, *94*, 7700.

(54) Wilkinson, P. G. *Can. J. Phys.* **1956**, *34*, 596.

(55) Dragomir, I. C.; Measey, T. J.; Hagarman, A. M.; Schweitzer-Stenner, R. *J. Phys. Chem. B* **2006**, *110*, 13235.

(56) Dreuw, A.; Head-Gordon, M. *Chem. Phys. Lett.* **2006**, *426*, 231 and references therein.